Hindawi
International Journal of Antennas and Propagation
Volume 2018, Article ID 8903139, 16 pages
https://doi.org/10.1155/2018/8903139

Review Article

RF Energy Harvesting for Ubiquitous, Zero Power Wireless Sensors

Warda Saeed, Nosherwan Shoaib, Hammad M. Cheema, and Muhammad U. Khan

Research Institute for Microwave and Millimeter-Wave Studies (RIMMS), National University of Sciences and Technology (NUST), Islamabad, Pakistan

Correspondence should be addressed to Nosherwan Shoaib; nosherwan.shoaib@seecs.edu.pk

Received 15 September 2017; Revised 24 October 2017; Accepted 31 January 2018; Published 22 April 2018

Academic Editor: N. Nasimuddin

This paper presents a review of wireless power transfer (WPT) followed by a comparison between ambient energy sources and an overview of different components of rectennas that are used for RF energy harvesting. Being less costly and environment friendly, rectennas are used to provide potentially inexhaustible energy for powering up low power sensors and portable devices that are installed in inaccessible areas where frequent battery replacement is difficult, if not impossible. The current challenges in rectenna design and a detailed comparison of state-of-the-art rectennas are also presented.

1. Introduction

The last decade has witnessed an unprecedented development in the field of wireless power transfer (WPT). However, the history of WPT which started with microwave power transmission (MPT) dates back to as far as the nineteenth century [1]. In the1880s, the experiments were carried out by Heinrich Hertz in order to prove the Maxwell's theory [2]. Subsequently, in the 1960s, Brown performed WPT experiments during World War II using high efficiency microwave technologies which were based on radar remote sensing and wireless communications [1]. The first rectenna was developed by R. George in 1963 using an array of 28 half-wave dipole-receiving antennas, each of which was connected to a bridge rectifier made using four 1N82G point-contact semiconductor diodes [3]. This rectenna, operating between 2 and 3 GHz, had an efficiency of 50% and 40% at output powers of 4 W and 7 W DC, respectively. The DC outputs very low due to the low power handling capability of the diodes, rendering this rectenna unsuitable for an ambitious target of powering up a helicopter rotor. Due to the low efficiency of the developed rectenna and the problem of most of the power being reflected at the antenna-diode interface, an impedance-matching network consisting of a plane array of rods was employed for improving the efficiency. More specifically, using 4480 1N82G diodes and the matching network, a much higher output power of 270 W was harvested which was apt for powering the helicopter rotor. Subsequently, on July1, 1964, a successful microwave-powered helicopter flight was made using the developed rectenna [3].

Nowadays, several renewable energy resources are being utilized to obtain the holy grail of never-ending green energy supply. For example, RF energy, solar energy, thermal energy, and wind energy sources are available to serve different purposes based on diverse requirements. Table 1 compares these energy resources using parameters such as power density, output voltage, availability, weight parameters, and the advantages and disadvantages of the solar, thermal, and ambient RF energy and piezoelectric energy sources [4]. The least power density of the ambient RF waves is due to its dissipation as heat and absorption by materials in the environment. Solar energy is only available during the daytime while thermal and RF energy are continuously available. The maximum output voltage is produced from piezoelectric energy harvesting that relies on vibrations (i.e., mechanical movement) generated through activity which are then converted to corresponding electrical energy. Solar, thermal, and piezoelectric energy require large area for energy harvesting while RF energy harvesting depends on distance

Table 1: Comparison between available ambient sources [4].

Energy sources/ parameters	Solar energy	Thermal energy	Ambient RF energy	Piezoelectric energy	
Power density	100 mW/cm^2	60 μW/cm^2	0.0002–1 μW/cm^2	Vibration 200 μW/cm^3	Push button 50 μJ/N
Output	0.5 V (single Si cell) 1.0 V (single a-Si cell)	—	3-4 V (open circuit)	10–25 V	100–10000 V
Available time	Daytime (4–8 Hrs)	Continuous	Continuous	Activity dependent	Activity dependent
Weight	5–10 g	10–20 g	2-3 g	2–10 g	1-2 g
Pros	Large amount of energy; well-developed technology	Always available	Antenna can be integrated onto frame; widely available	Well-developed technology; light weight	Well-developed technology; light weight; small volume
Cons	Needs large area; noncontinuous; orientation issue	Needs large area; low power; rigid and brittle	Distance dependent; depending on available power source	Needs large area; high variable output	High variable output; low conversion efficiency

Table 2: Characteristics of wireless power transmission (WPT) [1].

Receiver/characteristics	WPT via radio waves	Resonant coupling	Inductive coupling
Field	Electromagnetic (EM)	Resonance (electric, magnetic, or EM)	Magnetic
Receiver	Antenna	Resonator	Coil
Efficiency	Low to high	High	High
Distance	Short to long	Medium	Short
Power	Low to high	High	High
Safety	EM	None	Magnetic
Regulation	Radio wave	Under discussion	Under discussion

and the available RF sources in the environment. It is to be noted that, in comparison to others, technologies for harvesting thermal and ambient RF energy are lagging behind.

The RF energy harvesting is a "Green" self-sustainable operation which can potentially provide unlimited energy supply that can be used to remotely power up low power devices [5]. In particular, it helps to eliminate the need for a battery, which not only increases the cost, weight, and size of the device but the battery replacement is also costly and time-consuming especially when a lot of devices are spread over wide or inaccessible areas. Furthermore, it improves the reliability, portability, and user and environment friendliness and reduces the size and cost of the device. In addition, the finite lifetime of the electrical batteries is encouraging the researchers to explore further solutions in the field of RF energy harvesting, as acknowledged by Nikola Tesla, who described the freedom to transfer energy between two points without the need for a physical connection to a power source as an "all-surpassing importance to man" [6].

There are two main types of WPT mechanisms, namely, near-field and far-field systems. The former comprises the electromagnetic induction or magnetic resonance for wireless power transmission while the far-field WPT system uses antennas and rectifier circuitry for harnessing RF energy. Table 2 shows a comparison between the two mechanisms. Since the electromagnetic energy decays at the rate of 60 dB/decade in near-field region, therefore, the near-field systems are only suitable for indoor and short range (few centimetres) power transfer [4]. The electromagnetic induction can be used in various applications, for instance, in recharging the internal battery of the consumer electronics (electric toothbrush, wearables, and smart phones) while the magnetic resonant coupling between the two coils is used when the transmitter and the receiver are typically large. Energy obtained using high frequency (i.e., >1 GHz) RF waves is used to provide power to ultrahigh frequency (UHF) RFID and Zigbee devices in the range of 10 m [7]. However, it has a limitation on the power levels due to health and safety regulations (i.e., Radiocommunications (Electromagnetic Radiation—Human Exposure) Standard 2014) since the field strength of these waves can cause damage to human beings and other living creatures.

Few examples of wireless energy transfer applications are shown in Figure 1. A comparison of WPT techniques in terms of transmitted power and transmission range is elaborated in Figure 2. For home and office applications, the magnetic resonance and electromagnetic induction are preferred due to medium power transmission. The efficiency for RF power transfer is the least as compared to the electromagnetic induction and magnetic resonance and hence offers a number of research challenges [8].

Among the abovementioned WPT techniques, this review paper focuses on RF energy harvesting. The paper is organized as follows. Section 2 discusses the mechanism

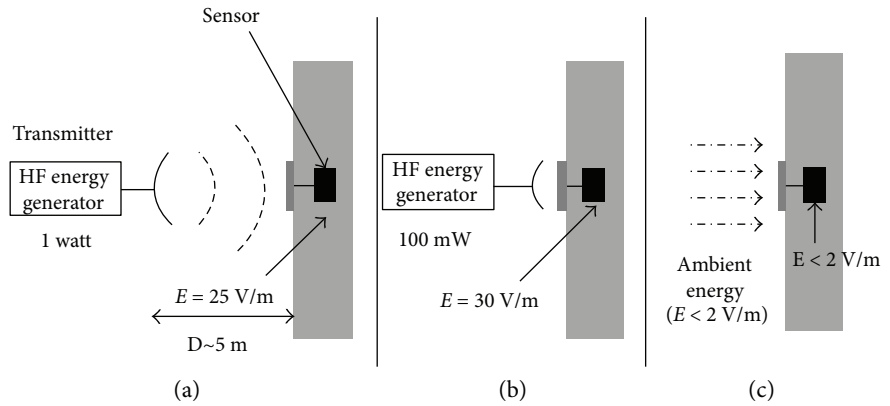

Figure 1: Example of wireless energy transfer to a remote sensor; (a) distant recharging; (b) proximity recharging (c) ambient energy harvesting [7].

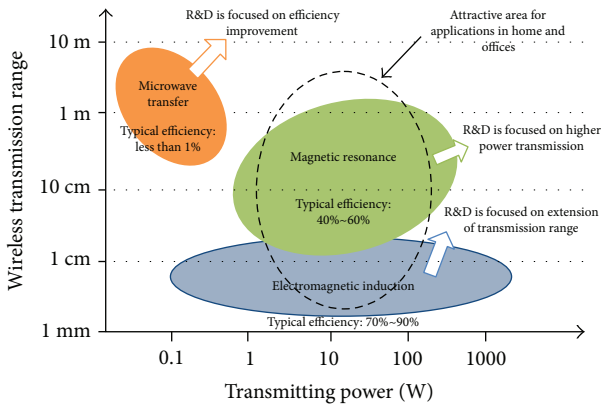

Figure 2: Comparison of various WPT technologies (efficiency here implies efficiency of whole power transfer system) [8].

of RF energy harvesting along with the various components of the rectenna system while Section 3 addresses the challenges faced during RF energy harvesting. Section 4 compares the published works followed by conclusions in Section 5.

2. Rectenna for RF Energy Harvesting

Ambient electromagnetic energy is present in abundance in the environment due to the increased usage of wireless technologies including WiMax, WLAN (2.4 GHz and 5.8 GHz), RFID (2.45 GHz, 5.8 GHz, and 24.125 GHz) cellular phones, 3G, 4G, Digital TV (DTV), GSM, radio, and microwave oven. The power levels of the common ambient RF sources are FM radio systems (transmitted power—few tens of kW), cell tower transmission (10 to 20 W per carrier), TV transmission (transmitted power—few tens of kW), Wi-Fi (2.45 GHz and 5.8 GHz), AM transmission (540–1600 kHz, transmitted power—few hundreds of kW), and mobile phones (transmitted power—1 to 2 W) [9]. The different RF energy sources can be categorized into three groups, namely, intentional sources, anticipated ambient sources, and unknown ambient sources. RF energy harvesting or RF energy scavenging can be used to directly power up battery-less systems and for battery activation. It can also be used for remote battery recharging, for instance, of a mobile phone, for powering up wireless sensor networks (WSN) and for waking up sensors in sleep mode [5]. This can be done by converting the EM waves in the ambience to a useable DC voltage with the help of a rectifying antenna called rectenna (i.e., antenna + rectifier).

The basic block diagram of a rectenna is shown in Figure 3. It comprises of a single or a combination of antennas, a bandpass or tunable filter (BPF), a broadband or multiband impedance matching network, a rectifier, and a low-pass filter that delivers the output to the load. The antenna is used for receiving the RF waves. The impedance-matching network is used to match the impedance of the antenna to the rectifying circuit for the maximum power transfer of RF energy to the rectifier. In addition, a matching network is used between the rectifier and the load to avoid impedance mismatches which can limit the maximum power available at the load. The rectifier converts the alternating voltage generated by the incident RF waves at the receiving antenna terminals to a DC voltage. A low-pass filter is used for obtaining ripple-free DC voltage across the connected load. In the following sections, these different components of the rectenna system will be discussed.

2.1. Receiving Antenna. The antenna is an integral part of the rectenna that should poses several requirements for harnessing the ubiquitous RF energy and converting it into a useful output DC voltage. Circularly polarized antennas are preferred in rectenna designs as they can receive both linearly and circularly polarized RF signals without any polarization loss. In contrast, linearly polarized antennas receive only half of the power of the circularly polarized wave and also suffer from polarization loss factor in capturing linearly polarized waves. This eventually results in the degradation of the overall efficiency of the rectenna. Furthermore, the antenna should be broadband so that it can receive all the ambient RF energy present in multiple frequency sources present in the surroundings. This is due to the fact that the power levels of the ambient signals are already in microwatts and more energy harvesting is required in order to get a sufficient output voltage for powering up ultralow power wireless sensor nodes. The antenna should also be miniaturized

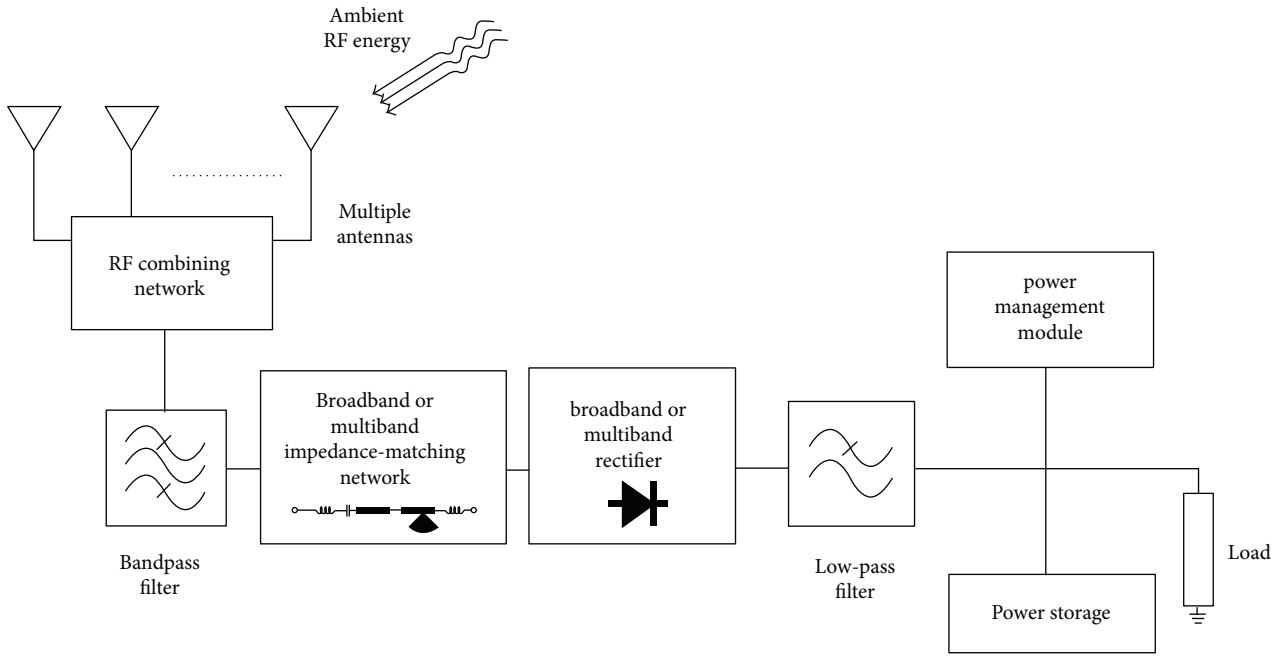

Figure 3: Block diagram of a rectenna.

and compact so that it can be used in portable and wireless charging applications.

In order to achieve more received power and an improved efficiency of the rectifier, both transmitting and receiving antennas should have high gain. One of the methods to increase the gain of the antenna is by making an antenna array. The array increases the RF power available at the rectifier input, but it also results in the increase of antenna size rendering it unsuitable for portable applications. Similarly, if the antenna is omnidirectional, then it can receive radiations from all the directions; however, its gain will be lower. These are some of the common trade-offs faced by researchers to achieve antennas that exhibit high efficiencies and output voltage, the ultimate goal of RF energy harvesting.

Several antenna types such as microstrip antenna, dipole, monopole, and Yagi-Uda antenna are used as the receiving antenna for RF energy harvesting. Most of the antenna designs found in literature are microstrip based owing to their low profile, compactness, light weight, high efficiency, low cost, easy fabrication, and conformity to planar and nonplanar surfaces. The most commonly used microstrip antennas are square, rectangular, and circular patch antennas mainly due to their low cross-polarization levels [5].

2.2. Matching Network. Impedance-matching network is an integral requirement in a rectenna design and was found between the antenna and the rectifier. The RF-DC conversion efficiency of rectenna greatly depends on its impedance-matching network. The design of matching network is challenging and requires several considerations. This is due to the fact that the input impedance values of rectifier circuit as well as antenna change with frequency. Further complexity is added due to the power-dependent behaviour of rectifier's input impedance; therefore, a broadband or multiband impedance-matching network needs to be designed for impedance matching over a wide range of frequencies and input power level.

The matching networks for the rectenna can be implemented using lumped elements or distributed microstrip lines. Each method of implementation has its own trade-offs. The quality factor Q of the lumped element-based matching circuit is lower as compared to the distributed line network, thus offering wider bandwidths. However, at frequencies higher than 1 GHz, the lumped components are not suitable due to the parasitic effects associated with them. Thus, microstrip line-based matching circuits are used at higher frequencies. The matching network is designed in such a way that the input impedance of the antenna is the complex conjugate of the input impedance of the rectifier circuit at a specified input power level.

A number of matching networks have appeared in literature for rectenna circuits. In [10], a dual-band bandpass impedance-matching network is proposed which is suitable for a load range of 1 kΩ to 10 kΩ. As shown in Figure 4, the proposed matching network is a sixth-order lumped element-matching network. The 4th order LC bandpass-matching topology is used for matching at the first frequency while the 2nd order modified L-network is used for impedance matching at the second frequency. An additional microstrip transmission line and a shunt radial stub are inserted between the inductors L3 and L4. The function of this additional section is to maintain the performance of the rectifier over a wide range of load values.

In [11], a broadband impedance matching is presented (Figure 5). The upper branch consists of a radial stub, a shorted stub, and a 6 nH chip inductor for impedance matching to 1.8 GHz and 2.5 GHz. The lower branch consists of a

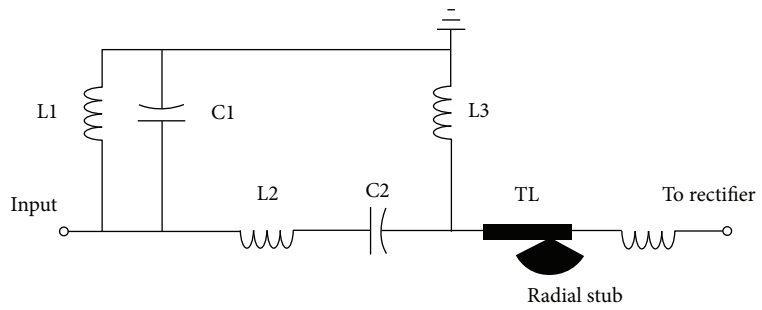

Figure 4: The proposed matching network with performance maintained for a range of load impedance from 1 kΩ to 100 kΩ [10].

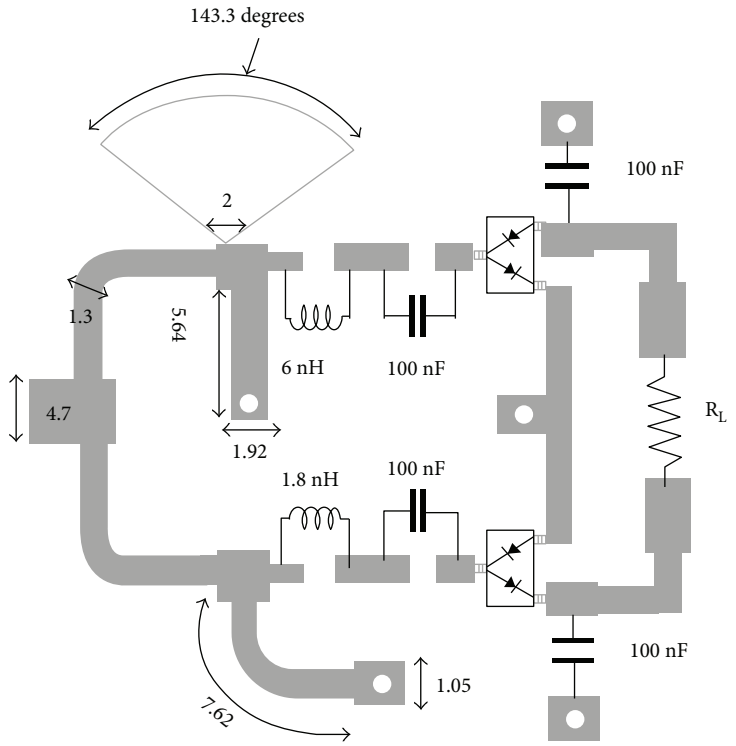

Figure 5: Topology of the proposed rectifier with a two-branch impedance-matching network. The parameters are in unit: mm [11].

bent shorted stub and a 1.8 nH chip inductor for matching to 2.1 GHz.

2.3. Rectifier. Rectifier, also called a charge pump, has three basic types: (i) basic rectifier, (ii) voltage doubler, and (iii) voltage multiplier. For rectenna application, a rectifier should have high RF to DC conversion efficiency. Typically implemented through one or more diodes, the choice of diode is of prime importance as it can be a major source of loss and its performance determines overall efficiency of the system. The power conversion efficiency of the rectifier mainly depends on the following: (i) series resistance of the diode (R_s), which determines the efficiency of the rectifier; (ii) zero-bias junction capacitance (C_{j0}) which affects the oscillation of harmonic currents through the diode; (iii) diode breakdown voltage, (V_{br}), which limits the power-handling capability of the diode; (iv) switching speed of the diode which should be fast so that it can follow a high frequency signal; (v) and low threshold voltage so that it can operate at low RF input power [12]. The maximum operating frequency of the diode is limited by the junction capacitance (C_j). The substrate and transmission line losses also contribute to the overall reduction of the efficiency of the energy-harvesting devices which depends on the type of substrate chosen and the length of the transmission line [6].

It is well known that diode produces harmonics and intermodulation products due to its nonlinear characteristics. Therefore, it reduces the energy that is to be converted to DC, thus reducing efficiency. The increased incident power results in increased losses due to the harmonics; thus, there is a trade-off between the harmonic generation, parasitic effects, reverse breakdown voltage, and the threshold voltage as shown in Figure 6 [6].

There are a number of commercially available diodes suitable for RF energy-harvesting applications keeping in view the low threshold voltage, low series resistance and

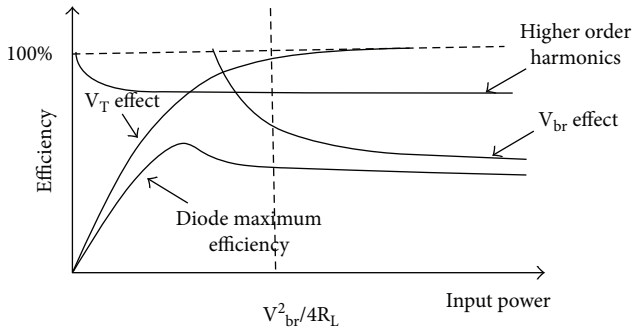

Figure 6: Relationship between efficiency, input power, and the losses in rectifier circuits [6].

junction capacitance, and high breakdown voltage. For instance, zero-bias Schottky diode HSMS2850 (by Agilent) has a low power-handling capability but also low threshold voltage of 150 mV, a low junction capacitance of 0.18 pF, and a breakdown voltage of 3.8 V for handling low powers. HSMS2860 has a higher power-handling capability, a threshold voltage of 350 mV, breakdown voltage of 7 V, and a series resistance of 6 Ω. HSMS2820 diodes are used with threshold voltages of 15 V and 6 Ω series resistance. HSMS8101 diode is also used which has a high power-handling capability but also low threshold voltage of 250 mV, a low junction capacitance of 0.26 pF, a series resistance of 6 Ω, and a breakdown voltage of around 7 V for handling low power. Therefore, HSMS8101 is preferred over HSMS2860 due to its lower threshold voltage and nearly same power-handling capability but for an input frequency range that is much higher than HSMS2860.

Skyworks diodes SMS7630-061, SMS7621-079F, and SMS7630-079LF have also been used in some of the published works. Among these, SMS7630-061 has a low power-handling capability, low threshold voltage of 180 mV, a low junction capacitance of 0.14 pF, a series resistance of 20 Ω, and a breakdown voltage of around 2 V. SMS7621-079F, on the other hand, has low power-handling capability but a slightly higher threshold voltage of 260 mV as compared to SMS7630-061, a low junction capacitance of 0.1 pF, a series resistance of 12 Ω, and a breakdown voltage of around 3 V. Lastly, SMS7630-079LF has a lower breakdown voltage as compared to the former two diodes while having a breakdown voltage of 2 V, a junction capacitance of 0.14 pF, and a high series resistance of 20 Ω.

For applications that require low power handling, a diode with minimum threshold voltage is preferred while a higher breakdown voltage diode is preferred for high power applications while the parameter junction capacitance and series resistance of the diode are of secondary importance. Table 3 lists some of the state-of-the-art rectifiers used in rectennas. They have been mostly designed at 900 MHz, 950 MHz, 915 MHz, 2.1 GHz, and 2.45 GHz ISM frequencies. The ambient RF signal power levels reaching the rectifier input are around −15 dBm, and it can be observed in Table 2 that the power levels of interest are in the range of −40 to 0 dBm where the performance of the rectifier is observed. In [13, 14], the rectifier circuit is implemented using CMOS transistors while the rest of the designs are implemented using silicon-based Schottky diodes. The maximum achieved efficiency is 78% for an input power of 23 dBm which is only possible when a dedicated source instead of an ambient source is used as the transmitter. Most of the rectifiers use HSMS28xx series diodes due to their better features as discussed earlier. In most cases, the diodes are used in voltage doubler configuration in order to increase the output voltage and power, resulting in an increased RF-DC conversion efficiency. CMOS 0.15 μm and 0.18 μm process transistors have also been used in rectifiers with a reported efficiency of 67.5% for −12.5 dBm input power with 1.8 V at the output of the rectifier.

2.4. Low-Pass Filter. A standard low-pass filter is typically utilized that consists of a capacitor connected in parallel with the load after the rectifier circuit. It is used to filter out the higher order harmonics from the DC component that is provided to the load (Figure 7).

2.5. Harmonic Suppression Networks. The suppression for the second and third order harmonics generated by the nonlinear diode in the rectifier is required to increase the overall efficiency of the rectifier. A low-pass filter at the input and output side can also be used for this purpose, but its design is complex due to the arbitrary terminated impedance. A matching network can also be designed for the fundamental frequency; however, this may add to the insertion loss and complexity of the overall device but also increases the size and cost of the rectenna. In order to suppress the second and third order harmonics, terminating networks are connected at the input and output of the rectifier. These terminating networks also serve as a matching circuit for the fundamental frequency. Figure 8(a) shows an example output-terminating network that behaves as an open circuit at the fundamental (f_0), second ($2f_0$), and third harmonic ($3f_0$) frequencies, thus reflecting all the harmonics and passing only the DC component to the load [18].

The electrical lengths of TL1 transmission line and TL2 are quarter wavelengths ($\lambda/4$) at f_0. From Figure 8(b), node A is short circuited for frequencies f_0 and $3f_0$. At the output of the diode, the short-circuit node A will be transformed to open circuit which suppresses f_0 and $3f_0$ components. Similarly, for $2f_0$, line TL2 will be open at node A. For $2f_0$, point B will be short circuited if TL4 is $\lambda/4$ long. The combined length of TL1 and TL3 is $3\lambda/4$ at $2f_0$ when the length of TL3 is also $\lambda/4$ at $2f_0$ (Figure 8(c)). At the diode's output, the node B becomes open, thus suppressing the second order harmonic [18].

Similarly, an example input termination network for the rectenna is shown in Figure 9(a). This network only allows f_0 to pass to the antenna and blocks the harmonics $2f_0$ and $3f_0$. The electrical lengths of transmission line TL6 is $\lambda/4$ at f_0. From Figure 9(b), there is a short circuit at node C for frequencies $2f_0$ [18]. The short-circuited node C will become open circuited at the input port of the diode for TL5 $\lambda/8$ at f_0. For $\lambda/4$ length of TL8 at $3f_0$, node D is short circuited (Figure 9(c)) while making the rest of the circuit ineffective at this frequency. For a combined $3\lambda/4$ length of TL5 and

Table 3: State-of-the-art rectifiers used in rectennas.

Reference	Operating frequency	Rectifier topology	Input power level of interest reaching the rectifier	Max. efficiency (%)	R_L (Ω)	V_{dc} (V)
[13]	950 MHz	0.5 μm and 0.18 μm CMOS process transistors	−22 dBm, −21 dBm	—	1 μW, 2 μW	—
[14]	953 MHz	Differential drive 0.18 μm CMOS bridge rectifier	−20 to 0 dBm	67.5 at −12.5 dBm	10 K	1.8
[15]	900 MHz–2.45 GHz	Bridge rectifier (HSMS2820)	−30 to 30 dBm	78 at 23 dBm	200	6.5 V
[16]	945 MHz	2 series diode (HSMS285C)	180 μW/cm^2	32 at 10 μW 52 at 100 μW	100 pF	2.2–4.5 V

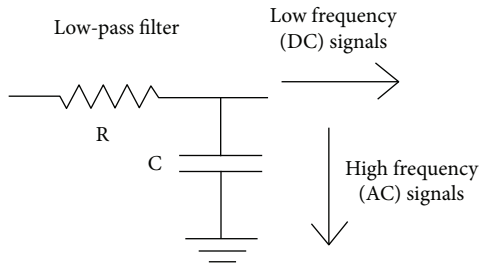

Figure 7: Low-pass filter topology [17].

TL7 at $3f_0$, the short condition at node D is transformed to open at the input of the diode. By setting the characteristic impedance of the lines TL5 and TL7 (Figure 9(d)), the impedance matching for the fundamental frequency can be implemented. The total length of TL5 and TL7 is $\lambda/4$ at $f_{0,}$ so the diode impedance can be transformed to 50 Ω using a quarter wave transformer and a TL8 $\lambda/4$ line to cancel the reactive part of the transformed impedance [18]. A different approach is adopted in [19], in which a ring antenna is used with inherent second harmonic rejection property. Similarly, in [20], a combination of an interdigitated capacitor and a chip capacitor not only performs impedance matching but also prevents higher order harmonics from reaching the antenna. As a result, the higher order harmonics return to the diode producing more DC power. Furthermore, the antenna performs a second order harmonic rejection and a radial stub is inserted between the antenna and rectifier for a third harmonic rejection. This eliminates the requirement of LPF thus resulting in a compact rectenna having reduced insertion loss at fundamental frequency. In [21, 22], a bandpass filter matches the impedance of the antenna to the impedance of the rectifier thus suppressing the reradiation of harmonics in free space. In addition, two cross-slots [22] and four right angle slits [23] are used to achieve harmonic rejection. In [24], the antenna is only matched at the fundamental frequency and intentionally mismatched at the harmonic frequencies eliminating the requirement of a separate filter, thus resulting in a compact size.

In [25], a double layer structure and an aperture-coupled fed antenna is used for harmonic suppression. For 5.8 GHz and 11.6 GHz, the simulated reflection coefficients are 40.2 dB and 0.13 dB, respectively. The DC filter at the output consists of three fan stubs having difference in their radius to stop the fundamental, second, and third order harmonics from reaching the load. Simulation results have shown that fan-shaped stub DC filter has more bandwidth as compared to the one having rectangular stub. In [11], an H-shaped slot filter on the ground plane and a flower-shaped slot filter on the antenna patch are used to suppress the second and third order harmonics generated by the diode (Figure 10).

Figure 11 shows a defected ground structure (DGS) in which a dumbbell-shaped slot on a rectangular patch antenna is present on the ground plane of the antenna. It suppresses the second and third harmonics which are at 4.9 GHz and 7.35 GHz, respectively [26].

2.6. DC-DC Boost Converter. A number of published papers have reported the use of a DC-DC converter in a rectenna. Since the DC-DC converter typically requires external DC power and also incurs some losses, it decreases the efficiency of the entire rectenna system. To overcome this issue, the use of boost converter between the rectifier and the storage element is proposed in some works. For instance, in [27], a switched capacitor DC-DC converter with three stages is used as reproduced in Figure 12. The converter chip was implemented using the IBM 8RF 0.13 μm CMOS process. The maximum output voltage is seven times the input voltage through the external capacitors.

In Figure 12, the top switches are made using nMOS transistors while the middle and the bottom switches are made by combining nMOS and pMOS transistors. This helps the accumulated charge on each capacitor to be transferred to the next stage with minimum loss. The capacitor arrays will charge the battery connected to the output of the DC-DC converter. This battery offers the highest specific charge storage capacity compared to any of the commercially available thin-film cell (>20 mAh·cm^{-2}). The commercially available secondary power cells require high recharge voltage, for example, lithium battery requires >3 V to recharge, while the cell that has been laboratory prepared in this paper requires only 1.2 V (open-circuit voltage of the battery after being fully charged) [27].

In [28], BQ25504 ultralow power boost converter with battery management is used to charge a capacitor which is used as a storage element. This boost converter is programmed for continuous charging of the storage capacitor. Similarly, in [29], a DC-DC boost converter design is proposed and connected as a load for the rectenna circuit. For a maximum power transfer from the rectenna to the boost converter with a high efficiency, it is ensured that the input

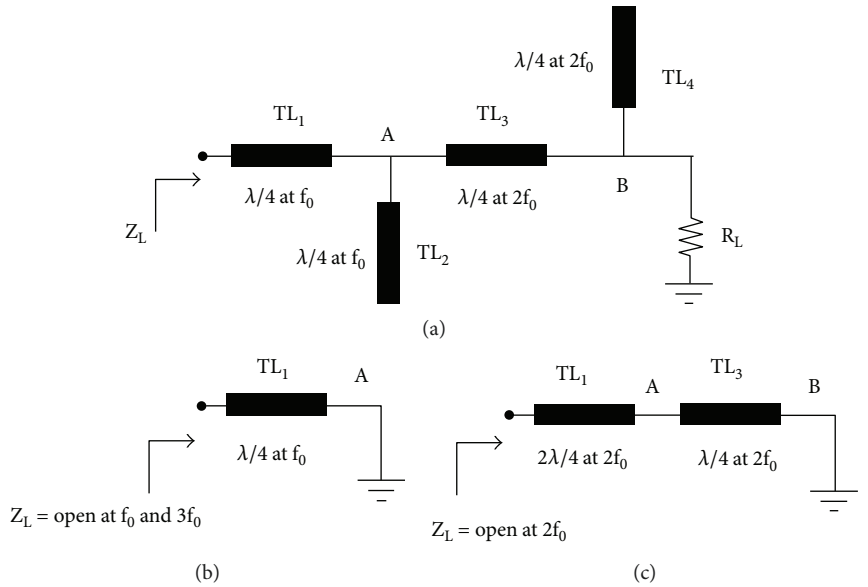

Figure 8: Example output termination network (a) output load network topology, (b) equivalent circuit at f_0 and $3f_0$, and (c) equivalent circuit at $2f_0$ [18].

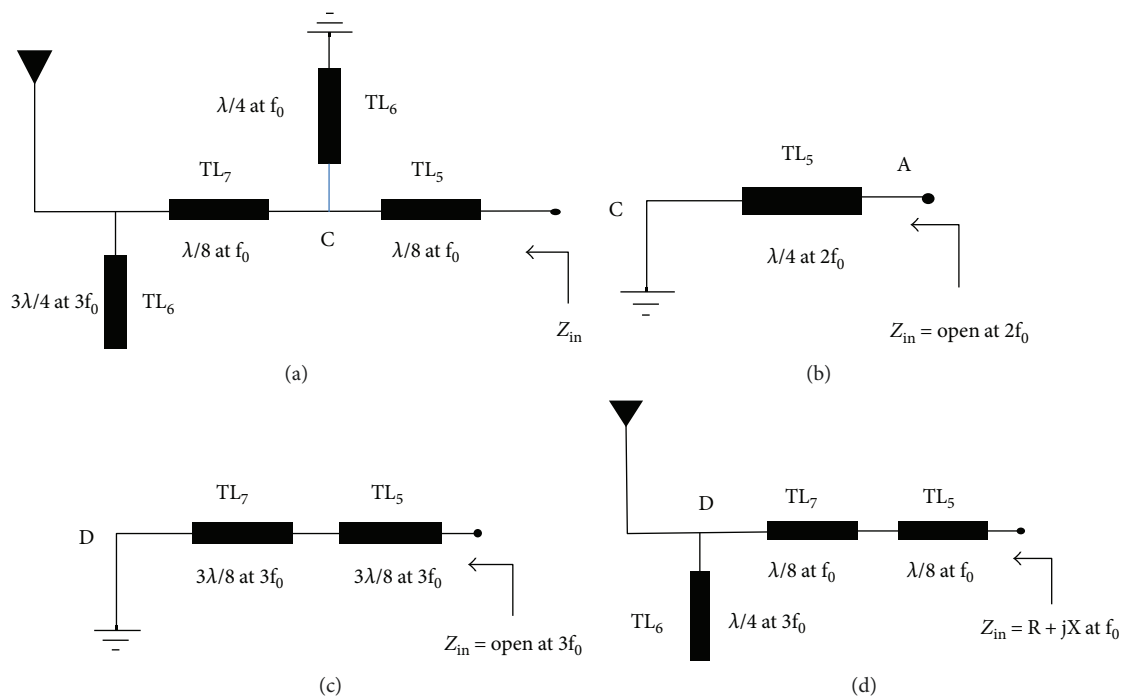

Figure 9: Proposed input termination network and its equivalent circuit: (a) input termination network, (b) equivalent circuit at $2f_0$, (c) equivalent circuit at $3f_0$, and (d) equivalent circuit at f_0 [18].

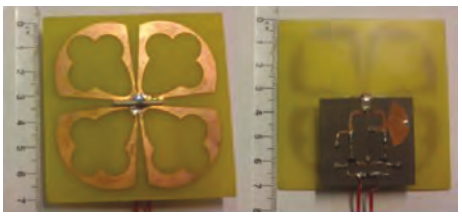

Figure 10: Front and back sides of the fabricated prototype in [11].

impedance of the boost converter emulates to the optimum load of the rectenna circuit as shown in Figure 13.

The power loss in the LTC1540 comparator oscillator circuit reduces the overall efficiency of the boost converter. This loss is the difference in the DC power measured at pin 7 (supply) to pin 8 (output). If the oscillator output is low (quiescent period), then the power loss is minimum and can be ignored; while for high oscillator output (active state), the power consumed by the oscillator is equal to the available

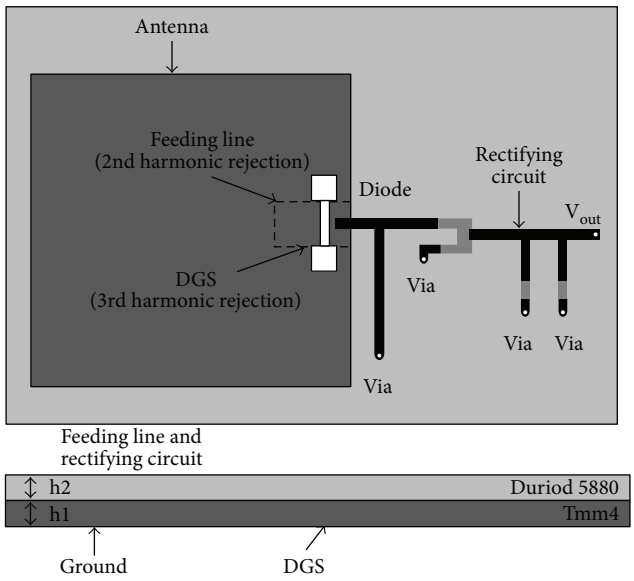

Figure 11: Antenna design for harmonic rejection [26].

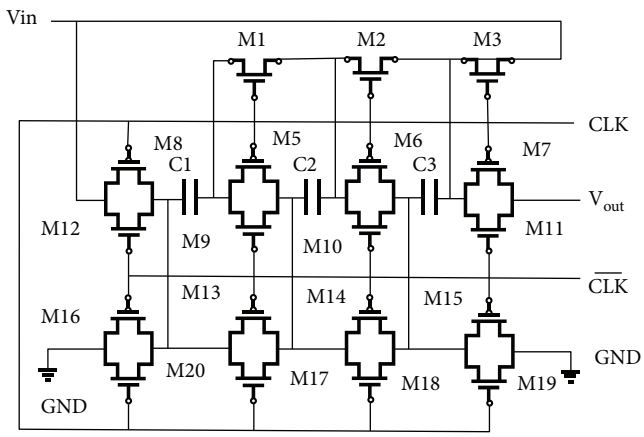

Figure 12: Schematic of the proposed DC-DC converter [27].

DC power at the boost converter output. Due to the large variations in the ambient RF input power, the maximum RF energy harvesting becomes a major challenge which can be addressed using a power management circuit which will deliver constant power to the load irrespective of the variations in the power levels at the input of the rectifier. On the same lines, in [30], a power management module is used comprising S882Z and AS1310 modules for boosting and regulating the output voltage as shown in Figure 14. The AS1310 is a hysteric step-up DC-DC converter from Austria Microsystems having ultralow quiescent current (<1 mA) so it can operate at a low DC voltage of 0.7 V, while S882Z from Seiko Instruments is an efficient charge pump IC for enhancing the step-up DC-DC converter performance. When a voltage of 0.3 V or higher is harvested, the oscillation circuit inside S882 starts itself and creates a clock signal. This CLK signal drives the charge pump circuit which steps up the harvested voltage and stores it in the low leakage CCPOUT capacitor. When the voltage on CCPOUT reaches a certain

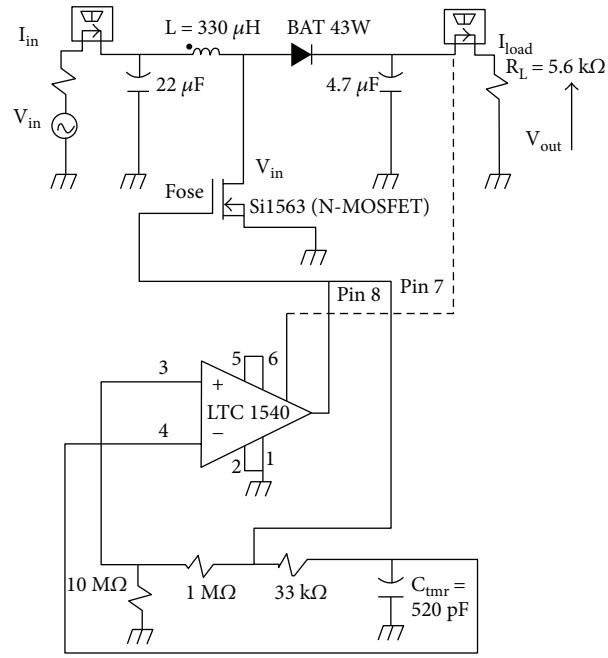

Figure 13: Schematic of the proposed DC-DC boost converter [29].

prespecified level, the power begins to flow to AS1310 which is then converted into a usable output DC voltage for powering up low power sensor.

The different parts of the rectenna, receiving antenna, impedance matching network, rectifier, low-pass filter, and DC-DC boost converter, are strongly interlinked, and a codesign approach is required to simulate and subsequently implement the whole system. The power received by the receiving antenna is passed on to the rectifier through an impedance-matching network so that the maximum power is transferred from the antenna to the rectifier. After the rectifier, a clean DC voltage is obtained through a low-pass filter and in some cases boosted up through a DC-DC converter for supporting meaningful applications. Therefore, all subparts of the system have their important role and a codesign approach can help in obtaining an overall efficient system.

3. Challenges for Ambient RF Energy Harvesting

Harvesting from ambient RF energy involves conflicting requirements and trade-offs between available power, range, frequency of operation, and gains of the transmitting and receiving antennas. In a typical far-field energy harvesting system in the well-known GSM and Wi-Fi frequency bands, the received RF power is very low since there is an inverse relation between the distance from the transmitter and the received power across the antenna terminals.

Another major challenge in rectenna systems is the design of a robust matching network. Since the impedance of the diode varies with frequency and input power levels, it is desired that the impedance-matching network should be broadband so that the frequency response remains flat for a wide range of frequencies. Furthermore, the rectifier should

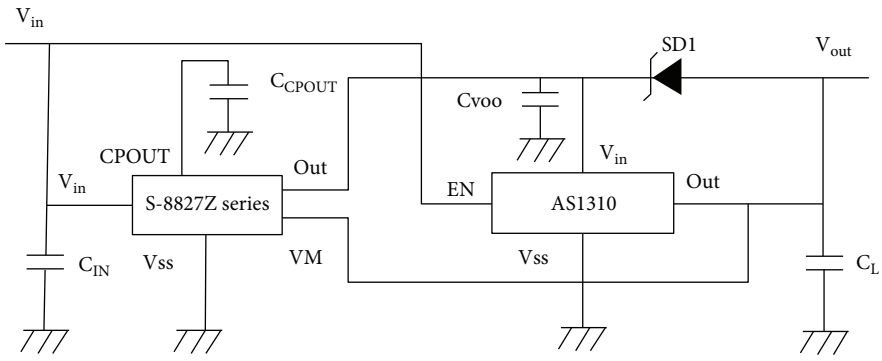

Figure 14: Power management circuit [30].

Table 4: Input RF power density levels of various ambient frequency bands in London [28].

Band	Frequencies (MHz)	Average S_{BA} (nW/cm^2)	Maximum S_{BA} (nW/cm^2)
DTV (during switch over)	470–610	0.89	460
GSM900 (MTx)	880–915	0.45	39
GSM900 (BTx)	925–960	36	1930
GSM1800 (MTx)	1710–1785	0.5	20
GSM1800 (BTx)	1805–1880	84	6390
3G (MTx)	1920–1980	0.46	66
3G (BTx)	2110–2170	12	240
Wi-Fi	2400–2500	0.18	6

have minimal losses and high conversion efficiency which requires challenging diode specifications of zero threshold voltage, high breakdown voltage, low series resistance, and junction capacitance [6].

To ascertain the abovementioned challenges, Table 4 shows, as an example, the input RF power densities for DTV, GSM900, GSM1800, 3G, and Wi-Fi bands outside the Northfields London underground station. Initially, the electric field strength measurements were recorded between 0.3 and 2.5 GHz using an Agilent N9912A FieldFox RF analyzer with a calibrated Aaronia BicoLOG 20300 omnidirectional antenna. The input RF power density (nW/cm^2) for a complete band is calculated by summing up the spectral peaks across the entire band. From the table, it can be seen that GSM1800 base station transmit band has the highest power density followed by GSM900 base station transmit band and 3G base transmit band, while the power density is minimum for DTV, GSM900, GSM1800, and 3G mobile transmit band. These power densities provide a starting point to the designer to identify suitable rectifier diodes [28].

4. State-of-the-Art Rectennas

A large body of published works on rectennas is present in literature. Table 5 summarizes the state-of-the-art designs comparing their frequency of operation, antenna type, antenna gain, rectifier topology, efficiency, and other important characteristics. It is noted that most of the designs focus on ISM bands of 2.45 and 5.8 GHz because of ample ambient energy available due to the wide use of Wi-Fi networks. Some rectenna designs have been made for the GSM900 and GSM1800 bands. These designs are more relevant to outdoor applications. Apart from these frequencies, a few rectennas have also been reported at 35 and 94 GHz [21].

The receiving antennas can be broadly categorized as omnidirectional and high-gain antennas which include dipole, folded dipole, monopole, ring antenna, Yagi-Uda, microstrip patch antenna, spiral antenna, SIW-backed cavity antenna, loop antenna, slot antenna, and PIFA antenna. These basic antenna structures have also been modified to obtain a wider bandwidth, higher gain, stable directional radiation pattern, antenna frequency configurability, and antenna miniaturization. The modified structures include tapered slot antenna, aperture-coupled patch antenna, miniaturized 2nd iteration Koch fractal microstrip patch antenna, circular patch antenna, hybrid Koch meander monopole, and E-shaped patch antenna. Furthermore, most of the antenna designs are either dual or circularly polarized with a very few linearly polarized as the latter causes polarization loss resulting in the deterioration of RF-DC conversion efficiency.

Among the designs listed in Table 5, the rectenna presented in [10] covers the most number of bands including 0.55, 0.75, 0.9, 1.85, 2.15, and 2.45 GHz with an efficiency of 67% at −5 dBm input power level to the rectifier. In [10], a bow tie-shaped planar cross-dipole omnidirectional antenna is proposed which is used due to its wide bandwidth of 400 MHz, bidirectional radiation pattern, and dual linear polarization characteristics. In order to further increase its bandwidth, the proposed design is converted to a frequency-independent log periodic cross-dipole antenna. However, it is designed neither for varying input power levels nor for varying frequencies and output loads which are the important parameters for maximizing RF-DC conversion efficiency. In order to harvest energy from a wide electromagnetic spectrum, many published works have employed modifications to standard antenna types to achieve desired performance. For instance, in [32], the high-gain antenna design is based on integration of a Yagi-Uda antenna with a wide-band dipole antenna. The antenna consists of a reflector and a single director placed nearby the driven dipole and provides the flexibility of acting as a broadband, dual-

Table 5: State-of-the-art rectennas.

Reference	Frequency	−10 dB impedance BW	Antenna type	Sensitivity/ antenna gain	Rectifier topology	Input power level to the rectifier	Max. efficiency (%)	R_L (Ω)	V_{dc} (V)	Polarization
[9]	2.67, 5.8 GHz	100 MHz, 690 MHz	Rectangular microstrip	8.6 dB, 9 dB	5-stage Dickson multiplier topology UMC180nm CMOS process	—	—	10^6	1.04	—
[10]	0.55, 0.75, 0.9, 1.85, 2.15, 2.45 GHz	550 MHz–2.5 GHz	Bow tie-shaped planar cross-dipole	3.1, 3.5, 4, 5, 4.9, 4.4 dB	SMS7630 voltage doubler	−30 to −5 dBm	67 at −5 dBm	10–75 kΩ	600 mV at 15 kΩ (outdoor) 400 mV at 3 kΩ (indoor)	Dual CP
[11]	—	700 MHz	Dipole antenna	2.4–4.15 dB	Two-stage/bridge voltage doubler (SMS7630)	−35 to 5 dBm	55 at −10 dBm	14700	250 m	Dual
[12]	900 MHz	—	Square-shaped folded dipole	80 mW/m^2 2 dBi	Voltage doubler (HSMS2862)	0–9 dBm	60 at 7 dBm	1000	2.4	—
[19]	35 GHz	—	Ring antenna	30000 μW/cm^2 4.54 dBi	Single Schottky diode (MA4E1317)	—	35 at 30000 μW/cm^2	50, 100, 200	0.45, 0.93, 1.73	Linear
[20]	5.8 GHz	150 MHz	Stepped impedance dipole	—	GaAs Schottky barrier diode (MA4E1317)	10–20 dBm	76 at 20 dBm	250	—	Linear
[21]	35 GHz, 94 GHz	82%, 41%	On chip=-tapered slot antenna 0.13 μm process	0–30 mW/cm^2 7.4, 6.4 dBi	full-wave rectifier	—	53, 37 at 30 mW/cm^2	100	0.38, 0.29	Linear
[22]	2.45 GHz	2100 MHz	Patch antenna	0.05–0.525 mW/cm^2	Series Schottky diode (HSMS2860)	—	63 at 0.525 mW/cm^2	1600	2.82	Dual circular
[24]	2.45 GHz	—	Patch antenna	0.22 μW/m^2 8.6 dBi	HSMS2852	−30 to 15 dBm	83 at 0 dBm	1400	3.75	—
[31]	2.45 GHz	—	Shorted ring slot antenna	20 μW/cm^2 5.25, 4.7 dB	Series diode (HSMS2850)	0–20 μW/cm^2	69 at 20 μW/cm^2	2500	1.1	Circular
[25]	5.78 GHz	—	Aperture-coupled patch	7 dBi	Series diode (HSMS2860)	17.78 dBm	63 at 13 dBm	900	3.1	Dual
[32]	900 MHz, 1800 MHz, 2.45 GHz	—	Modified Yagi-Uda antenna	3.26, 3.02, 6.88 dBi	Voltage multiplier (HSMS2852)	−15 dBm	46, 45, 25 at −15 dBm	50 k	0.84	—
[33]	2.45 GHz	137 MHz	Patch antenna	16500 μW/cm^2	Schottky Voltage doubler	20 dBm	70 at 20 dBm	1000	12	Circular
[34]	2.45 GHz	—	Square patch	—	Single series Schottky diode	0–15 dBm	75 at 15 dBm	200	—	—

Table 5: Continued.

Reference	Frequency	−10 dB impedance BW	Antenna type	Sensitivity/ antenna gain	Rectifier topology	Input power level to the rectifier	Max. efficiency (%)	R_L (Ω)	V_{dc} (V)	Polarization
[35]	2.45 GHz	750 MHz	Square aperture-coupled patch	—	SMS7630 voltage doubler	−20 dBm	15.7 at −20 dBm, 42.1 at −10 dBm	5000	0.9 m	Dual linear
[36]	5.8 GHz	12 MHz	Patch	3.4 dBi	Two Schottky diode HSMS2862	−10 to 16 dBm	—	—	72.5 m at 16 dBm	Circular
[37]	2.45 GHz	—	Patch	0.15 mW/cm^2 6.2 dB	Bridge rectifier with 4 Schottky diodes	0–16 dBm	61 at 10 dBm	1050	3.64	Linear
[38]	2.45 GHz	25 MHz	Miniaturized 2nd iteration Koch fractal microstrip patch antenna	3.8 dBi	Two-stage Dickson voltage doubler (HSMS2852) Schottky diode	−25-10 dBm	70 at 2 dBm	13000	1.6	—
[39]	2.45 GHz	100 MHz	Square aperture-coupled patch	1.5 μW/m^2 7.7 dB	2x voltage doubler	−19.2 dBm	38.2 at −19.2 dBm	6200	96 m	Dual linear
[40]	900 MHz	121 MHz	EM-coupled square microstrip antenna	9.1 dB	Schottky diode single-stage voltage doubler	−1 to −10 dB	—	100 k	2.78	—
[41]	900 MHz	285 MHz	E-shaped patch antenna	—	7 stage voltage doubler (HSMS2850)	−40 to 5 dBm	—	STLM20 temperature sensor	2.14	—
[30]	2.45 GHz	—	Planar patch antenna	0.5 dBi	Modified Greinacher rectifier	−40 to −20 dBm	—	10 k	1.764	—
[42]	2.45 GHz	—	Patch antenna	—	Shunt diode (SMS7630-079LF)	−20 to −40 dBm	33.7 at −11.2 dBm	1500	7.36	—
[43]	1800 MHz, 2100 MHz	400 MHz	Quasi-Yagi antenna	455 μW/m^2 10.9, 13.3 dBi	Series Avago HSMS2852 diode	−30 to −5 dBm	40 at −20 dBm (two-tone input)	5000	224 m	Linear
[44]	915 MHz, 2.45 GHz	—	Slot-loaded folded dipole	1 μW/cm^2, 1.87, 2.45 dBi	Series diode (SMS7630)	−40 to 0 dBm	37, 30 at −9 dBm	2.2 k	—	Circular
[45]	900 MHz	—	One-sided slot antenna	−0.7 dBi	4 stage Cockcroft-Walton circuit (HSMS286Y)	−10 dBm	58.7 at −10 dBm	10 M	2.9	—
[46]	915 MHz	—	Rectangular patch antenna	10.67, 10.30 dBi	3 stage Dickson rectifier	0–10 dBm	40 at 10 dBm	LED	3	Linear
[47]	2.4 GHz	140 MHz	Circular slotted truncated corner square patch	4.6 dBic	Single-stage Dickson rectifier	0 dBm	28.9 at 0 dBm	600 k	1.5	Circular
[48]	2.45 GHz	—	Patch antenna	8 dBic	A pair of HSMS282C diodes	−10 to 20 dBm	82.3 at 22 dBm	1000	11.42	Dual circular

Table 5: Continued.

Reference	Frequency	−10 dB impedance BW	Antenna type	Sensitivity/ antenna gain	Rectifier topology	Input power level to the rectifier	Max. efficiency (%)	R_L (Ω)	V_{dc} (V)	Polarization
[49]	24 GHz	2 GHz	SIW cavity-backed patch antenna	10 mW/cm^2 12.6 dBc	Series MA4E1317 diode	0–13 dBm	24 at 10 mW/cm^2	Open	1.25 at 20 dBm	Circular
[50]	2.45 GHz	—	Cross-slot coupled square patch	5.5 dBis	Parallel combination of 2 diodes (SMS7630-079LF)	−50 to −10 dBm	37.7 at −15 dBm	1500	189 m	Dual circular
[51]	2.45 GHz	140 MHz	Patch antenna	295.3 μW/cm^2 7.45 dBi	Shunt single diode (HSMS2860)	−20 to 20 dBm	78 at 12 dBm	850	—	Dual linear
[52]	2.45 GHz	400 MHz	Slot antenna	10 dBi	Voltage doubler (HSMS2862)	0–20 dBm	72.5 at 13 dBm	900	3.5	—
[53]	900 MHz	135 MHz	Differential microstrip antenna	8.5 dBi	Voltage doubler	−10 to 15 dBm	65.3 at 3 dBm	3000	1.80	
[54]	900 MHz, 1800 MHz, 2.1 GHz, 2.45 GHz,	—	Dipole	6 dBi	Differential voltage doubler (MSS20-141)	−20 to 0 dBm	84 at −15 dBm	11 k	1.2	—
[55]	35 GHz	4 GHz	Rectangular microstrip patch antenna	19 dBi	Shunt GaAs Schottky diode MA4E1317	0–8.45 dBm	67 at 8.45 dBm	1000	2.18	Linear
[56]	850 MHz–1.94 GHz	1090 MHz	Broadband-bent triangular monopole	2 dBi	Voltage doubler	0–10 dBm	60 at 980 MHz, 17 at 1800 MHz	500	1.38 at 4.3 K	—

band, or multiband antenna by easily tuning the antenna due to which it is being used in the design of a rectenna. Similarly, in [49], SIW cavity technique is used to achieve a gain boost of 2.3 dBc as well as improving the 3 dB axial ratio bandwidth three times compared to a standard CP array with no cavity-backing. Furthermore, CPW transmission lines are used owing to their several advantages like low radiation loss, high circuit density, low dispersion, and easy integration to with active and passive elements. In general, the antennas that employ the CPW slot are wideband and are easy to match to the rectifier impedance. As a conclusion from Table 5, it is observed that patch antennas are the most suitable option for RF energy harvesting due to their light weight, low cost, and the advantage of being conformal with planar and nonplanar structures. On the other hand, monopole and dipole antennas have also been used but have low gain with an omnidirectional radiation pattern whereas slot antennas have smaller size and higher bandwidth as compared to conventional patch antennas. Yagi-Uda antennas have high gain and a directional radiation pattern albeit with large size whereas spiral/ring antennas have also been used due to their large bandwidth and good radiation characteristics.

Mostly, the diodes in a voltage doubler configuration are used in order to boost the output voltage for meaningful applications such as powering wireless sensor nodes. Some of the common diode models include MA4E1317, SMS760, and HSMS28xx which are predominantly GaAs-based Schottky diodes.

5. Conclusions

The appeal of harnessing energy out of thin air is attractive enough to garner interest from researchers despite the obvious challenges of low power levels, low RF-DC conversion efficiency, and broadband matching. In the era of Internet of Things where low power sensors are expected to be ubiquitous and aptly dubbed as "smart dust," RF energy harvesting provides a potentially low cost and long lasting alternative to batteries, especially for applications for remote and/or inaccessible areas. Efficient multiband/broadband antennas, rectifiers tolerant to input power and frequency variations, and multiband/broadband-matching networks are few of the ongoing areas of focus, overcoming which tangible use of RF energy harvesting for real-life applications will be possible in the near future.

Conflicts of Interest

The authors declare that there is no conflict of interest regarding the publication of this paper.

References

[1] N. Shinohara, "Power without wires," *IEEE Microwave Magazine*, vol. 12, no. 7, pp. S64–S73, 2011.

[2] H. J. Visser and R. J. M. Vullers, "RF energy harvesting and transport for wireless sensor network applications: principles and requirements," *Proceedings of the IEEE*, vol. 101, no. 6, pp. 1410–1423, 2013.

[3] W. C. Brown, "The history of power transmission by radio waves," *IEEE Transactions on Microwave Theory and Techniques*, vol. 32, no. 9, pp. 1230–1242, 1984.

[4] S. Kim, R. Vyas, J. Bito et al., "Ambient RF energy-harvesting technologies for self-sustainable standalone wireless sensor platforms," *Proceedings of the IEEE*, vol. 102, no. 11, pp. 1649–1666, 2014.

[5] S. Shrestha, S. K. Noh, and D. Y. Choi, "Comparative study of antenna designs for RF energy harvesting," *International Journal of Antennas and Propagation*, vol. 2013, Article ID 385260, 10 pages, 2013.

[6] C. R. Valenta and G. D. Durgin, "Harvesting wireless power: survey of energy-harvester conversion efficiency in far-field, wireless power transfer systems," *IEEE Microwave Magazine*, vol. 15, no. 4, pp. 108–120, 2014.

[7] V. Marian, C. Vollaire, J. Verdier, and B. Allard, "Potentials of an adaptive rectenna circuit," *IEEE Antennas and Wireless Propagation Letters*, vol. 10, pp. 1393–1396, 2011.

[8] H. Shoki, "Issues and initiatives for practical deployment of wireless power transfer technologies in Japan," *Proceedings of the IEEE*, vol. 101, no. 6, pp. 1312–1320, 2013.

[9] M. Arrawatia, M. S. Baghini, and G. Kumar, "RF energy harvesting system at 2.67 and 5.8GHz," in *2010 Asia-Pacific Microwave Conference*, pp. 900–903, Yokohama, Japan, 2010, IEEE.

[10] C. Song, Y. Huang, P. Carter et al., "A novel six-band dual CP rectenna using improved impedance matching technique for ambient RF energy harvesting," *IEEE Transactions on Antennas and Propagation*, vol. 64, no. 7, pp. 3160–3171, 2016.

[11] C. Song, Y. Huang, J. Zhou, J. Zhang, S. Yuan, and P. Carter, "A high-efficiency broadband rectenna for ambient wireless energy harvesting," *IEEE Transactions on Antennas and Propagation*, vol. 63, no. 8, pp. 3486–3495, 2015.

[12] S. Ladan, N. Ghassemi, A. Ghiotto, and K. Wu, "Highly efficient compact rectenna for wireless energy harvesting application," *IEEE Microwave Magazine*, vol. 14, no. 1, pp. 117–122, 2013.

[13] S. Mandal and R. Sarpeshkar, "Low-power CMOS rectifier design for RFID applications," *IEEE Transactions on Circuits and Systems I: Regular Papers*, vol. 54, no. 6, pp. 1177–1188, 2007.

[14] K. Kotani, A. Sasaki, and T. Ito, "High-efficiency differential-drive CMOS rectifier for UHF RFIDs," *IEEE Journal of Solid-State Circuits*, vol. 44, no. 11, pp. 3011–3018, 2009.

[15] V. Marian, B. Allard, C. Vollaire, and J. Verdier, "Strategy for microwave energy harvesting from ambient field or a feeding source," *IEEE Transactions on Power Electronics*, vol. 27, no. 11, pp. 4481–4491, 2012.

[16] G. Singh, R. Ponnaganti, T. V. Prabhakar, and K. J. Vinoy, "A tuned rectifier for RF energy harvesting from ambient radiations," *AEU - International Journal of Electronics and Communications*, vol. 67, no. 7, pp. 564–569, 2013.

[17] "Learning about electronics, "low pass filter"," http://www.learningaboutelectronics.com/Articles/Low-pass-filter.php.

[18] G. Chaudhary, P. Kim, Y. Jeong, and J. H. Yoon, "Design of high efficiency RF-DC conversion circuit using novel termination networks for RF energy harvesting system," *Microwave and Optical Technology Letters*, vol. 54, no. 10, pp. 2330–2335, 2012.

[19] Y.-J. Ren, M.-Y. Li, and K. Chang, "35 GHz rectifying antenna for wireless power transmission," *Electronics Letters*, vol. 43, no. 11, pp. 602-603, 2007.

[20] W.-H. Tu, S.-H. Hsu, and K. Chang, "Compact 5.8-GHz rectenna using stepped-impedance dipole antenna," *IEEE Antennas and Wireless Propagation Letters*, vol. 6, pp. 282–284, 2007.

[21] H.-K. Chiou and I. S. Chen, "High-efficiency dual-band on-chip rectenna for 35- and 94-GHz wireless power transmission in 0.13-μm CMOS technology," *IEEE Transactions on Microwave Theory and Techniques*, vol. 58, pp. 3598–3606, 2010.

[22] Z. Harouni, L. Cirio, L. Osman, A. Gharsallah, and O. Picon, "A dual circularly polarized 2.45-GHz rectenna for wireless power transmission," *IEEE Antennas and Wireless Propagation Letters*, vol. 10, pp. 306–309, 2011.

[23] F.-J. Huang, T.-C. Yo, C.-M. Lee, and C.-H. Luo, "Design of circular polarization antenna with harmonic suppression for rectenna application," *IEEE Antennas and Wireless Propagation Letters*, vol. 11, pp. 592–595, 2012.

[24] H. Sun, Y.-x. Guo, M. He, and Z. Zhong, "Design of a high-efficiency 2.45-GHz rectenna for low-input-power energy harvesting," *IEEE Antennas and Wireless Propagation Letters*, vol. 11, pp. 929–932, 2012.

[25] X.-X. Yang, C. Jiang, A. Z. Elsherbeni, F. Yang, and Y. Q. Wang, "A novel compact printed rectenna for data communication systems," *IEEE Transactions on Antennas and Propagation*, vol. 61, no. 5, pp. 2532–2539, 2013.

[26] Z. Harouni, L. Osman, and A. Gharsallah, "Efficient 2.45 GHz rectenna design with high harmonic rejection for wireless power transmission," *International Journal of Computer Science Issues*, vol. 5, p. 7, 2010.

[27] W. Zhao, K. Choi, S. Bauman, Z. Dilli, T. Salter, and M. Peckerar, "A radio-frequency energy harvesting scheme for use in low-power ad hoc distributed networks," *IEEE Transactions on Circuits and Systems II: Express Briefs*, vol. 59, no. 9, pp. 573–577, 2012.

[28] M. Pinuela, P. D. Mitcheson, and S. Lucyszyn, "Ambient RF energy harvesting in urban and semi-urban environments," *IEEE Transactions on Microwave Theory and Techniques*, vol. 61, no. 7, pp. 2715–2726, 2013.

[29] C. Mikeka and H. Arai, "Design issues in radio frequency energy harvesting system," in *Sustainable Energy Harvesting Technologies - Past, Present and Future*, InTech, Europe, 2011.

[30] U. Olgun, C.-C. Chen, and J. L. Volakis, "Design of an efficient ambient WiFi energy harvesting system," *IET Microwaves, Antennas & Propagation*, vol. 6, no. 11, pp. 1200–1206, 2012.

[31] H. Takhedmit, L. Cirio, S. Bellal, D. Delcroix, and O. Picon, "Compact and efficient 2.45 GHz circularly polarised shorted ring-slot rectenna," *Electronics Letters*, vol. 48, no. 5, pp. 253-254, 2012.

[32] S. Keyrouz, H. J. Visser, and A. G. Tijhuis, "Multi-band simultaneous radio frequency energy harvesting," in *2013 7th European Conference on Antennas and Propagation (EuCAP)*, pp. 3058–3061, Gothenburg, Sweden, 2013, IEEE.

[33] T.-C. Yo, C. M. Lee, C. M. Hsu, and C. H. Luo, "Compact circularly polarized rectenna with unbalanced circular slots," *IEEE Transactions on Antennas and Propagation*, vol. 56, no. 3, pp. 882–886, 2008.

[34] A. Douyère, J. D. Lan Sun Luk, and F. Alicalapa, "High efficiency microwave rectenna circuit: modelling and design," *Electronics Letters*, vol. 44, no. 24, pp. 1409-1410, 2008.

[35] G. A. Vera, A. Georgiadis, A. Collado, and S. Via, "Design of a 2.45 GHz rectenna for electromagnetic (EM) energy scavenging," in *2010 IEEE Radio and Wireless Symposium (RWS)*, pp. 61–64, New Orleans, LA, USA, 2010, IEEE.

[36] T. M. Chiam, L. C. Ong, M. F. Karim, and Y. X. Guo, "5.8GHz circularly polarized rectennas using Schottky diode and LTC5535 rectifier for RF energy harvesting," in *2009 Asia Pacific Microwave Conference*, pp. 32–35, Singapore, 2009, IEEE.

[37] H. Takhedmit, B. Merabet, L. Cirio et al., "A 2.45-GHz low cost and efficient rectenna," in *Proceedings of the Fourth European Conference on Antennas and Propagation*, pp. 1–5, Barcelona, Spain, 2010, IEEE.

[38] U. Olgun, C.-C. Chen, and J. L. Volakis, "Low-profile planar rectenna for batteryless RFID sensors," in *2010 IEEE Antennas and Propagation Society International Symposium*, pp. 1–4, Toronto, ON, Canada, 2010, IEEE.

[39] A. Georgiadis, G. Vera Andia, and A. Collado, "Rectenna design and optimization using reciprocity theory and harmonic balance analysis for electromagnetic (EM) energy harvesting," *IEEE Antennas and Wireless Propagation Letters*, vol. 9, pp. 444–446, 2010.

[40] M. Arrawatia, M. S. Baghini, and G. Kumar, "RF energy harvesting system from cell towers in 900MHz band," in *2011 National Conference on Communications (NCC)*, pp. 1–5, Bangalore, India, 2011, IEEE.

[41] N. M. Din, C. K. Chakrabarty, A. B. Ismail, K. K. A. Devi, and W.-Y. Chen, "Design of RF energy harvesting system for energizing low power devices," *Progress In Electromagnetics Research*, vol. 132, pp. 49–69, 2012.

[42] H. Hong, X. Cai, X. Shi, and X. Zhu, "Demonstration of a highly efficient RF energy harvester for Wi-Fi signals," in *2012 International Conference on Microwave and Millimeter Wave Technology (ICMMT)*, pp. 1–4, Shenzhen, China, 2012, IEEE.

[43] H. Sun, Y. X. Guo, M. He, and Z. Zhong, "A dual-band rectenna using broadband Yagi antenna array for ambient RF power harvesting," *IEEE Antennas and Wireless Propagation Letters*, vol. 12, pp. 918–921, 2013.

[44] K. Niotaki, S. Kim, S. Jeong, A. Collado, A. Georgiadis, and M. M. Tentzeris, "A compact dual-band rectenna using slot-loaded dual band folded dipole antenna," *IEEE Antennas and Wireless Propagation Letters*, vol. 12, pp. 1634–1637, 2013.

[45] H. Kanaya, S. Tsukamaoto, T. Hirabaru, D. Kanemoto, R. K. Pokharel, and K. Yoshida, "Energy harvesting circuit on a one-sided directional flexible antenna," *IEEE Microwave and Wireless Components Letters*, vol. 23, no. 3, pp. 164–166, 2013.

[46] F. Xie, G. M. Yang, and W. Geyi, "Optimal design of an antenna array for energy harvesting," *IEEE Antennas and Wireless Propagation Letters*, vol. 12, pp. 155–158, 2013.

[47] K. Agarwal, T. Mishra, M. F. Karim, M. O. Chuen, Y. X. Guo, and S. K. Panda, "Highly efficient wireless energy harvesting system using metamaterial based compact CP antenna," in *2013 IEEE MTT-S International Microwave Symposium Digest (MTT)*, pp. 1–4, Seattle, WA, USA, 2013, IEEE.

[48] J.-H. Chou, D. B. Lin, K. L. Weng, and H. J. Li, "All polarization receiving rectenna with harmonic rejection property for wireless power transmission," *IEEE Transactions on Antennas and Propagation*, vol. 62, no. 10, pp. 5242–5249, 2014.

[49] S. Ladan, A. B. Guntupalli, and K. Wu, "A high-efficiency 24 GHz rectenna development towards millimeter-wave energy harvesting and wireless power transmission," *IEEE*

Transactions on Circuits and Systems I: Regular Papers, vol. 61, no. 12, pp. 3358–3366, 2014.

[50] W. Haboubi, H. Takhedmit, J. D. Lan Sun Luk et al., "An efficient dual-circularly polarized rectenna for RF energy harvesting in the 2.45 GHz ISM band," *Progress In Electromagnetics Research*, vol. 148, pp. 31–39, 2014.

[51] H. Sun and W. Geyi, "A new rectenna with all-polarization-receiving capability for wireless power transmission," *IEEE Antennas and Wireless Propagation Letters*, vol. 15, pp. 814–817, 2016.

[52] M.-J. Nie, X. X. Yang, G. N. Tan, and B. Han, "A compact 2.45-GHz broadband rectenna using grounded coplanar waveguide," *IEEE Antennas and Wireless Propagation Letters*, vol. 14, pp. 986–989, 2015.

[53] M. Arrawatia, M. S. Baghini, and G. Kumar, "Differential microstrip antenna for RF energy harvesting," *IEEE Transactions on Antennas and Propagation*, vol. 63, no. 4, pp. 1581–1588, 2015.

[54] V. Kuhn, C. Lahuec, F. Seguin, and C. Person, "A multi-band stacked RF energy harvester with RF-to-DC efficiency up to 84%," *IEEE Transactions on Microwave Theory and Techniques*, vol. 63, no. 5, pp. 1768–1778, 2015.

[55] A. Mavaddat, S. H. M. Armaki, and A. R. Erfanian, "Millimeter-wave energy harvesting using 4×4 microstrip patch antenna array," *IEEE Antennas and Wireless Propagation Letters*, vol. 14, pp. 515–518, 2015.

[56] M. Arrawatia, M. Baghini, and G. Kumar, "Broadband bent triangular omnidirectional antenna for RF energy harvesting," *IEEE Antennas and Wireless Propagation Letters*, vol. 15, pp. 36–39, 2016.